PHYSICAL REVIEW D **91,** 123519 (2015)

Improved cosmological model fitting of Planck data with a dark energy spike

Chan-Gyung Park

Division of Science Education and Institute of Fusion Science, Chonbuk National University, Jeonju 561-756, Republic of Korea

(Received 27 February 2015; published 12 June 2015)

The Λ cold dark matter (ΛCDM) model is currently known as the simplest cosmology model that best describes observations with a minimal number of parameters. Here we introduce a cosmology model that is preferred over the conventional ΛCDM one by constructing dark energy as the sum of the cosmological constant Λ and an additional fluid that is designed to have an extremely short transient spike in energy density during the radiation-matter equality era and an early scaling behavior with radiation and matter densities. The density parameter of the additional fluid is defined as a Gaussian function plus a constant in logarithmic scale-factor space. Searching for the best-fit cosmological parameters in the presence of such a dark energy spike gives a far smaller chi-square value by about 5 times the number of additional parameters introduced and narrower constraints on the matter density and Hubble constant compared with the best-fit ΛCDM model. The significant improvement in reducing the chi square mainly comes from the better fitting of the Planck temperature power spectrum around the third ($\ell \approx 800$) and sixth ($\ell \approx 1800$) acoustic peaks. The likelihood ratio test and the Akaike information criterion suggest that the model of a dark energy spike is strongly favored by the current cosmological observations over the conventional ΛCDM model. However, based on the Bayesian information criterion which penalizes models with more parameters, the strong evidence supporting the presence of a dark energy spike disappears. Our result emphasizes that the alternative cosmological parameter estimation with even better fitting of the same observational data is allowed in Einstein's gravity.

DOI: 10.1103/PhysRevD.91.123519 PACS numbers: 98.80.-k, 95.36.+x

I. INTRODUCTION

Finding the simplest model that best describes astronomical observations is one of the primary aims in cosmology. Until now, the best concordance model with the minimal number of parameters is currently known as the Λ cold dark matter (ΛCDM) model with the cosmological constant Λ as dark energy and CDM as the dominant dark matter [1–3].

Many efforts have been made to develop a cosmology model that is better than the conventional ΛCDM model. Determining which model is preferable is a problem of model selection. The standard approach used in the model selection is that one constrains the new model with data using the likelihood method and checks whether or not it is supported over the previous best model based on statistical criteria. In usual cases, the new candidate cosmology model has more free parameters than the ΛCDM model, while it often gives a better fitting of observational data. However, simply adding more parameters and getting a smaller chi square (or larger likelihood) does not make the relevant model better. In order for a new cosmology model to be ranked as better than the ΛCDM model, it should pass through at least one of the model selection criteria such as the likelihood ratio test [4], the Akaike information criterion [5], the Bayesian information criterion [6], Bayesian evidence, and so on (see also Refs. [7–12] for applications in cosmology with brief reviews).

Although many dark energy models have been proposed, most of them give only a small improvement in fitting the observational data compared with the ΛCDM model and do not pass through the model selection criteria with high significance, implying that the ΛCDM model is the final winner in the model selection process [10–21].

Recently, Park *et al.* [22] investigated the observational effect of early episodically dominating dark energy based on a minimally coupled scalar field with the Albrecht-Skordis potential, where the dark energy density transiently becomes strong during a short period of time. They showed that the presence of the early episodic dark energy can affect the cosmological parameter estimation significantly and concluded that the recent Planck data strongly favor the ΛCDM model because only a limited amount of dark energy with episodic nature is allowed. In this paper, we introduce a fluid version of the early transiently dominating dark energy model with a similar episodic nature. Our dark energy model is designed to have a transient spike in the energy density during an extremely short period and an early scaling behavior with radiation and matter density. We show that our dark energy model gives a significantly improved fit to the recent observational data with different parameter constraints, and thus it is preferred over the best-fit ΛCDM model based on some

model selection criteria. Through the example of the dark energy spike model, we show that the alternative parameter estimation with even better fitting of the same observational data is allowed in Einstein's gravity.

This paper is organized as follows. Section II describes the fluid-based dark energy spike model with a transient variation in dark energy density and presents numerical calculations of the background evolution of this model. In Sec. III, observational effects of the dark energy spike are investigated using recent observational data, such as the cosmic microwave background radiation (CMB) data from the Planck satellite and the baryonic acoustic oscillation (BAO) data from the large-scale structure surveys. The cosmological parameters constrained with observations are compared in the presence or absence of the dark energy spike. In Sec. IV, we compare our dark energy model with the conventional ΛCDM model based on some statistical criteria used in model selection. The discussion and conclusion are presented in Sec. V. Throughout this paper, we set $c \equiv 1$ and $8\pi G \equiv 1$.

II. A FLUID-BASED DARK ENERGY SPIKE MODEL

The quintessence-based early episodically dominating dark energy model proposed in Ref. [22] is on a solid theoretical footing, but it has its limitations. First, it is not easy to control the onset, strength, and duration of the transient dark energy because the behavior of dark energy strongly depends on potential parameters and initial conditions. Second, the scalar-field-based dark energy model cannot accommodate a dark energy *spike*—a transient and abrupt variation of dark energy density during an extremely short period—which inevitably induces the crossing of the phantom divide ($w = -1$) in the dark energy equation of state (see Figs. 1 and 2), since the quintessence model theoretically does not allow $w = -1$ crossing.

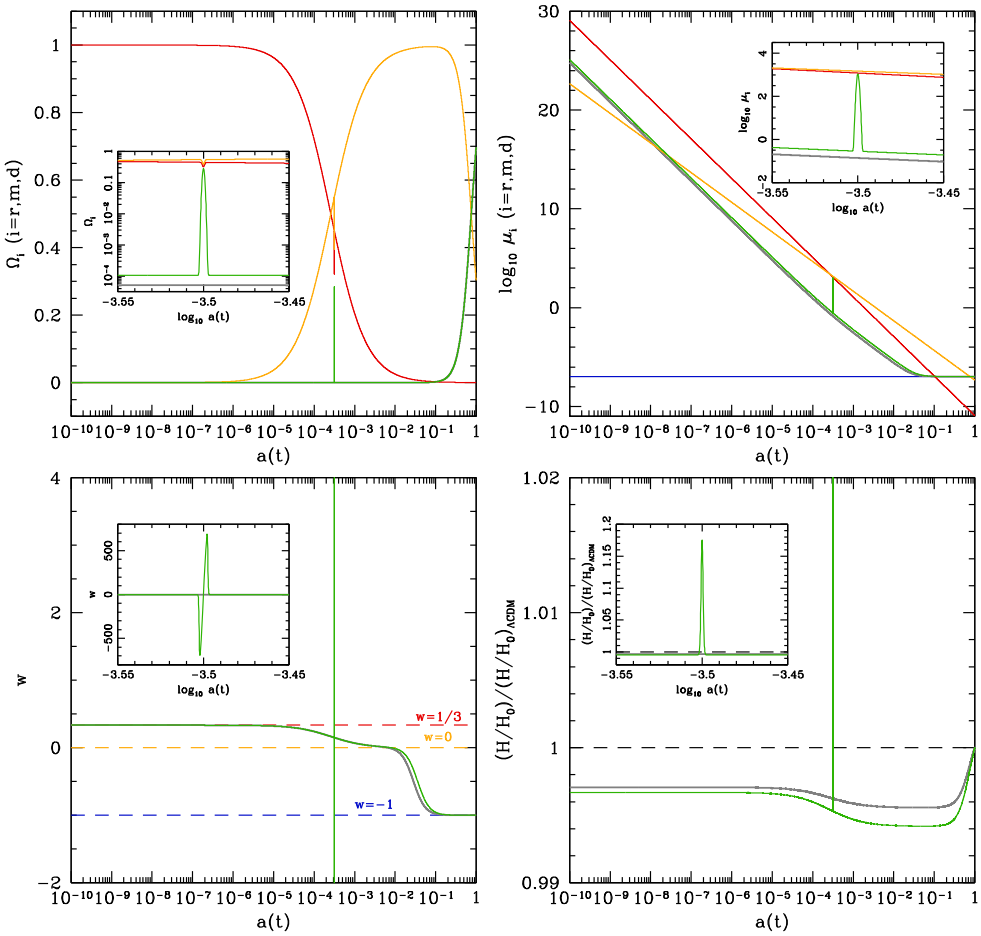

FIG. 1 (color online). Evolution of the density parameters (Ω_i; $i = r, m, d$), energy densities (μ_i), dark energy equation of state (w), and normalized Hubble parameter divided by the ΛCDM prediction $[(H/H_0)/(H/H_0)_{\Lambda CDM}]$ in the best-fit spike-DE model with $\log_{10} a_c = -3.5$, $A = 0.28$, $B = 1.1 \times 10^{-4}$, $\sigma = 1.5 \times 10^{-3}$. In the top panels, the behaviors of the radiation (r), matter (m), and dark energy (d) components are shown as red, yellow, and green curves, respectively. The energy density due to the cosmological constant in the best-fit ΛCDM model is shown as a blue curve (top right panel). In all panels, grey curves represent the results of the scaling-DE model with $B = 5.2 \times 10^{-5}$. The precise values of the model parameters used in the numerical calculation are presented in Table I.

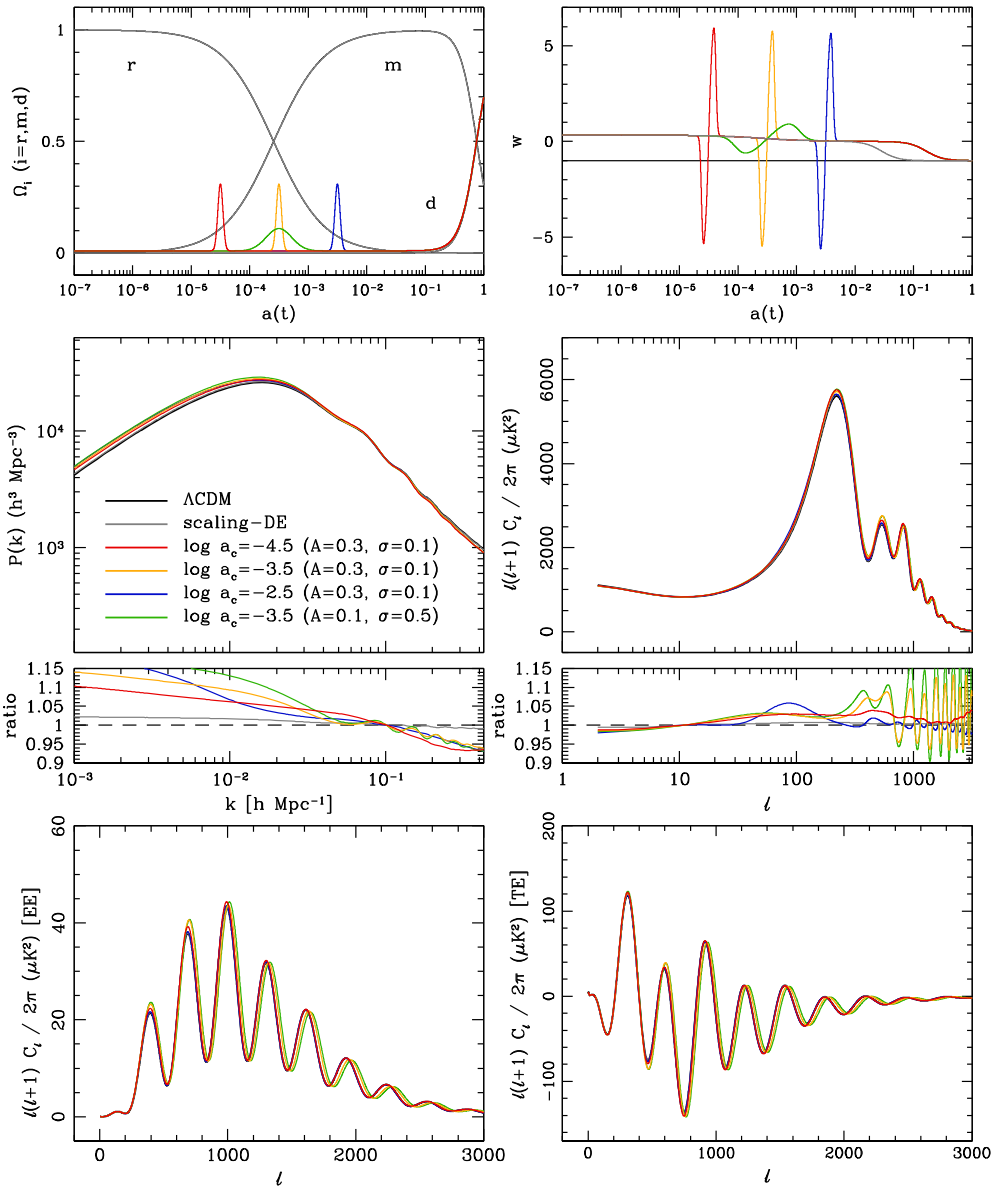

FIG. 2 (color online). Evolution of the density parameters (Ω_i; $i = r, m, d$) and dark energy equation of state (w) (top), and the power spectra of the baryonic matter density (middle left), CMB temperature fluctuations (middle right), and polarization (bottom panels) in the spike-DE models (with $A = 0.3$, $B = 0.01$, $\sigma = 0.1$) for $\log_{10} a_c = -4.5$ (red), -3.5 (yellow), and -2.5 (blue curves). Green curves indicate the case of $\log_{10} a_c = -3.5$ but with weaker and broader dark energy domination ($A = 0.1$, $\sigma = 0.5$). Other cosmological parameters are the same as those in the best-fit ΛCDM model. Gray curves represent the results of the scaling-DE model and black curves those of the best-fit ΛCDM model. For the matter and CMB temperature anisotropy power spectra, the ratio of the dark energy model power spectrum to the ΛCDM one is also shown. The matter power spectra are normalized to the ΛCDM model prediction at $k = 0.1h$ Mpc^{-1}, while the CMB anisotropy power spectra $\ell = 10$.

In the quintessence model of Ref. [22], the level of dark energy domination (e.g., near the radiation-matter equality) should be sufficiently small to consistently match the recent Planck CMB data, which implies that the ΛCDM limit is strongly favored by the current observations. However, the duration of the transient dark energy was rather long ($\Delta \log_{10} a \approx 1$) in that model. In this paper, we consider the possibility that the strong dark energy domination with an extremely short duration ($\Delta \log_{10} a \ll 1$) may be favored by the observations, providing a better fit to the data, which is our main motivation for the present work. It will be shown in Sec. III that the model of the dark energy spike near the radiation-matter equality with a duration of $\Delta \log_{10} a \approx 10^{-3}$ can achieve a significant improvement in data fitting over the ΛCDM model, while those with longer durations cannot, as in the quintessence model.

Here we introduce a fluid model of early dark energy that is easy to handle numerically and allows for a dark energy

spike, which the quintessence version cannot accommodate. In fact, our fluid model is not the exact theoretical counterpart of the quintessence model, but rather a simple version that mimics the overall behavior of transient dark energy of the scalar field model. However, we will see that the early dark energy of both models show similar observational effects in the power spectra of density perturbations (see Fig. 2).

In the conventional ΛCDM model, we add a new fluid (denoted as x) with a transient spike in energy density. We assume that the dark energy density parameter (Ω_x) is represented as the sum of a Gaussian function and a constant in logarithmic scale-factor space,

$$\Omega_x(a) = \frac{\mu_x}{3H^2} = A \exp\left[-\frac{(\ln a - \ln a_c)^2}{2\sigma^2}\right] + B, \quad (1)$$

where μ_x is the energy density of the additional fluid, $a(t)$ is the cosmic scale factor normalized to unity at present, $H = \dot{a}/a$ is the Hubble parameter at epoch a (with a dot as a time derivative), and A, a_c, and σ are interpreted as the amplitude (strength), temporal position, and duration of the dark energy spike, respectively. The constant term B denotes the level of early dark energy that exists from the beginning of the Universe and is responsible for the scaling evolution where the dark energy density follows that of the dominant fluid. In this paper, we incorporate the x fluid and the cosmological constant Λ into the effective fluid of dark energy (DE). The behavior of dark energy in our model shows early scaling evolution with the radiation and matter densities, with a sudden dark energy spike at a particular epoch and the late-time acceleration phase due to the cosmological constant. From here on, we call the dark energy model with both the scaling and transient behaviors the spike-DE model, and the model with only the scaling behavior the scaling-DE model. Note that both the ΛCDM model ($A = 0$, $B = 0$) and the scaling-DE model ($A = 0$ and $B \geq 0$) are nested within the spike-DE model.

In the presence of the x fluid, the squared Hubble parameter normalized with the present value is given by

$$\left(\frac{H}{H_0}\right)^2 = \frac{\Omega_{r0}a^{-4} + \Omega_{m0}a^{-3} + \Omega_{\Lambda 0} + \Omega_{K0}a^{-2}}{1 - \Omega_x(a)}, \quad (2)$$

where the subindices r, m, and K represent the radiation, matter, and spatial curvature, respectively, and the subindex zero indicates the present value. We assume that the x fluid satisfies the continuity equation, $\dot{\mu}_x = -3H(\mu_x + p_x)$. The pressure of the x fluid is given by

$$p_x = 3H^2\Omega_x\left(-1 - \frac{2\dot{H}}{3H^2} - \frac{\Omega_x'}{3\Omega_x}\right), \quad (3)$$

where

$$\Omega_x'(a) = \frac{d\Omega_x}{d\ln a} = -\frac{\ln a - \ln a_c}{\sigma^2}(\Omega_x - B) \quad (4)$$

and

$$\frac{\dot{H}}{H^2} = \frac{1}{1-\Omega_x}\left\{\left(-2\Omega_{r0}a^{-4} - \frac{3}{2}\Omega_{m0}a^{-3} - \Omega_{K0}a^{-2}\right) \times \left(\frac{H_0}{H}\right)^2 + \frac{1}{2}\Omega_x'\right\}. \quad (5)$$

Throughout this paper, we consider a spatially flat universe ($\Omega_{K0} = 0$). The equation of state of the effective dark energy fluid (denoted by a subindex d) becomes

$$w = \frac{p_d}{\mu_d} = -1 - \frac{2\dot{H}\Omega_x}{3H^2(\Omega_x + \Omega_\Lambda)} - \frac{\Omega_x'}{3(\Omega_x + \Omega_\Lambda)}, \quad (6)$$

where $\mu_d = \mu_x + \Lambda$, $p_d = p_x - \Lambda$, and $\Omega_\Lambda = \Lambda/(3H^2)$. The dark energy density parameter ($\Omega_d = \Omega_x + \Omega_\Lambda$) has three asymptotic values: $\Omega_d \simeq A + B$ at the onset of the dark energy spike ($a = a_c$), $\Omega_d \simeq B$ before and after the onset ($|a - a_c| \gg 0$) and before the late-time acceleration ($a \ll a_0$), and $\Omega_d \simeq B + \Omega_\Lambda$ during the acceleration phase ($a \approx a_0 \gg a_c$).

Figure 1 shows the evolution of the density parameters, energy densities, the dark energy equation of state, and the Hubble parameter in the spike-DE model where a strong dark energy spike occurs at $a = 10^{-3.5}$ ($\ln a_c = -8.059$), together with those in the scaling-DE and ΛCDM models. As expected, the dark energy densities of the spike-DE (green) and scaling-DE (grey) models show scaling behaviors following radiation and matter sequentially. The model parameters have been adopted as the best-fit ones obtained with the recent observational data (see Sec. III for details). In the spike-DE model, the dark energy equation of state experiences a change of about 3 orders of magnitude when crossing the phantom divide twice during the occurrence of the dark energy spike. Considering 95.4% (2σ) confidence limits of the Gaussian shape of the spike, it lasts for about 600 years ($3.153 \times 10^{-4} < a < 3.172 \times 10^{-4}$).

III. OBSERVATIONAL CONSTRAINTS ON THE DARK ENERGY SPIKE MODEL

We probe the observational signatures of our spike-DE model by considering both the scalar- and tensor-type perturbations in a system of multiple components for radiation, matter, and the effective dark energy fluid (the x fluid plus the cosmological constant). For this aim, we have modified the publicly available CAMB/COSMOMC package (version of Dec. 13 2013) [23,24] to include the evolution of the background and the perturbation of the effective dark energy fluid, and we explore the allowed ranges of the conventional cosmological parameters in the presence of a dark energy spike using the Planck CMB data

together with other external data sets. For the evolution of the perturbed density and velocity of the x fluid, the parametrized post-Friedmann prescription for the dark energy perturbations is used to allow for multiple crossings of the phantom divide ($w = -1$) in the time-dependent dark energy equation of state [25]. Following the Planck team's analysis, we assume the current CMB temperature as $T_0 = 2.7255$ K and the effective number of neutrinos as $N_\nu = 3.046$ with a single massive eigenstate of mass $m_\nu = 0.06$ eV [2].

Figure 2 shows how the transient dark energy domination affects the background evolution and power spectra of the perturbed densities. We choose three spike-DE models of a strong and narrow spike ($A = 0.3$, $B = 0.01$, $\sigma = 0.1$) with $\log_{10} a_c = -4.5$ (red), -3.5 (yellow), and -2.5 (blue curves) and one model of a weak and broad dark energy domination ($A = 0.1$, $B = 0.01$, $\sigma = 0.5$) for the case of $\log_{10} a_c = -3.5$ (green curves). Note that the dark energy equation of state for the latter model does not show a $w = -1$ crossing as in the quintessence model. The observational effects of the dark energy spike are very similar to those seen in the scalar-field-based model (Fig. 3 of Ref. [22]). For the same strength, the dark energy spike has weak observational effects if it occurs before the radiation-matter equality (the case of $\log_{10} a_c = -4.5$). However, a dark energy spike near (or after) that epoch induces significant deviations from the ΛCDM model prediction. As was already seen in Ref. [22], in the case of $\log_{10} a_c = -3.5$—which corresponds to a dark energy spike near the radiation-matter equality—we observe highly oscillatory features at small angular scales in the CMB temperature anisotropy power spectrum and a strong deviation from the ΛCDM model at all angular scales in the polarization power spectra. Though the effects are much weaker, the same is true in the case of $\log_{10} a_c = -2.5$. Besides, the CMB temperature power spectra for the strong and narrow spike (yellow curve) and for the weak and broad one (green curve) at $\log_{10} a_c = -3.5$ suggest that both the strength and duration of transient dark energy have similar and significant effects on the small-scale power spectrum. Compared with the CMB anisotropy, however, the matter power spectrum is less sensitive to the presence of the dark energy spike.

We use the CMB data obtained with Planck [26], which is a combination of the CMB temperature anisotropy angular power spectrum up to small angular scales ($\ell = 2500$) and the Wilkinson Microwave Anisotropy Probe 9-year polarization data [27]. We use four Planck CMB likelihood data sets (2013 version), `Lowlike` for the low-ℓ temperature and polarization likelihood covering $\ell = 2$–32, `Commander` for the low-ℓ temperature-only likelihood covering $\ell = 2$–49, `CamSpec` for the high-ℓ temperature-only likelihood with $\ell = 50$–2500 [28], and `Lensing` for the lensing effect [29]. As the external data derived from the large-scale structure observations, we also use the BAO data points measured by the Sloan Digital Sky Survey Data Release 7 (DR7) [30], the Baryon Oscillation Spectroscopic Survey Data Release 9 (DR9) [31], the 6dF Galaxy Survey [32], and the Wiggle Z surveys [33].

With CMB and BAO data, we have constrained the parameter space of the spatially flat ΛCDM, scaling-DE, and spike-DE models that are favored by the observations. We limit our investigation by considering a spike-DE model with a dark energy spike occurring near the radiation-matter equality era ($\log_{10} a_c = -3.5$); see Fig. 1. The reason for choosing such an epoch is that the transient domination of dark energy near the radiation-matter equality has the greatest effect on the evolution of the density perturbations, inducing a highly oscillatory feature in the angular power spectrum of the temperature fluctuations at high multipoles (see Fig. 2). The free conventional cosmological parameters are $\Omega_{b0}h^2$, $\Omega_{c0}h^2$, h, τ, n_s, r, and $\ln[10^{10}A_s]$, where Ω_{b0} (Ω_{c0}) is the baryon (CDM) density parameter at the current epoch, h is the normalized Hubble constant with

TABLE I. Best-fit cosmological parameters of the spatially flat ΛCDM, scaling-DE, and spike-DE models.

Parameter	ΛCDM	Scaling-DE	Spike-DE
A	0	0	0.28360
B	0	5.1736×10^{-5}	1.0662×10^{-4}
$\log_{10} a_c$	⋯	⋯	−3.5
σ	⋯	⋯	1.4604×10^{-3}
$100\Omega_b h^2$	2.21632	2.22226	2.19523
$\Omega_c h^2$	0.11827	0.11778	0.11777
h	0.67929	0.68130	0.68158
τ	0.09623	0.08908	0.08873
n_s	0.96550	0.96487	0.97147
r	0.00048	0.00046	0.01640
$\ln[10^{10}A_s]$	3.09985	3.08397	3.08691
t_0 (Gyr)	13.7992	13.7930	13.7983
$A_{100}^{\rm PS}$	178.3636	138.0731	140.2106
$A_{143}^{\rm PS}$	62.92783	50.31658	61.88821
$A_{217}^{\rm PS}$	118.6188	115.4876	126.9649
$A_{143}^{\rm CIB}$	6.620212	3.852115	5.640900
$A_{217}^{\rm CIB}$	25.52911	26.94230	23.30611
$A_{143}^{\rm tSZ}$	3.724382	8.408760	2.995350
$r_{143\times217}^{\rm PS}$	0.9075909	0.8956619	0.9206412
$r_{143\times217}^{\rm CIB}$	0.2190109	0.3866272	9.2171337×10^{-3}
$\gamma^{\rm CIB}$	0.5448702	0.5265283	0.5609424
c_{100}	1.000590	1.000599	1.000575
c_{217}	0.9963431	0.9962796	0.9968735
$\xi^{\rm tSZ\text{-}CIB}$	0.5315524	5.734012×10^{-4}	0.2737207
$A^{\rm kSZ}$	0.1122116	0.2684244	0.1527581
β_1^1	0.5376251	0.5772729	0.2189442

$H_0 = 100h$ kms^{-1} Mpc^{-1}, τ is the reionization optical depth, n_s is the spectral index of the primordial scalar-type perturbation, r is the ratio of tensor- to scalar-type perturbations, and A_s is the amplitude of the primordial curvature perturbations with $A_s = k^3 P_{\mathcal{R}}(k)/(2\pi^2)$ at the pivot scale $k_0 = 0.05$ Mpc^{-1}. The running of the spectral index is not considered. There are also several foreground and calibration parameters (see Table I and Ref. [2] for detailed descriptions of the parameters).

The free parameters of spike-DE model are A, B, and σ with a_c fixed [see Eq. (1)]. With the conventional and dark energy model parameters (except for a_c) all varying freely,

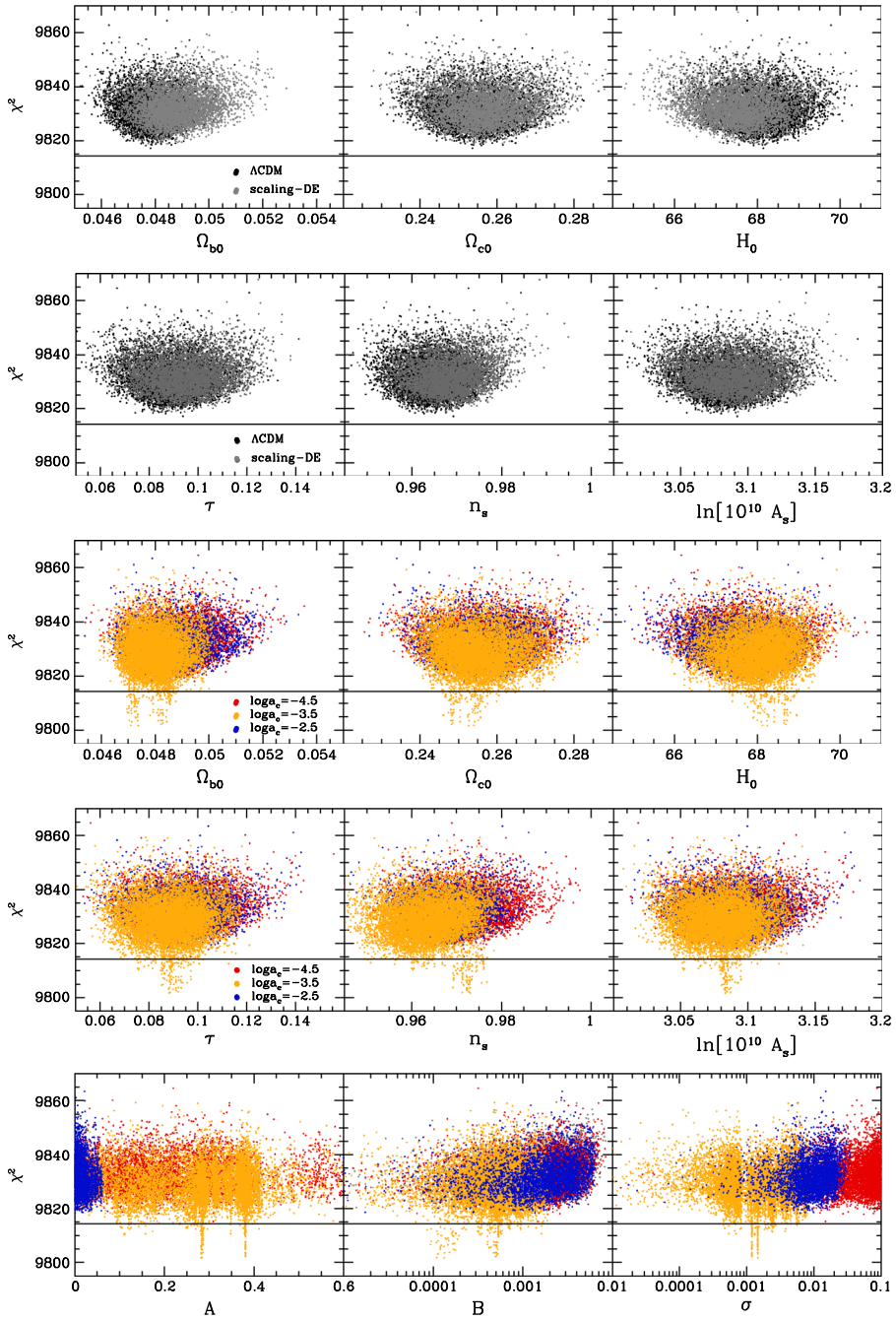

FIG. 3 (color online). Chi square versus free cosmological parameters from the unconverged trial MCMC chains of the ΛCDM (black), scaling-DE (grey), and three spike-DE models with fixed $\log_{10} a_c = -4.5$ (red), -3.5 (yellow), and -2.5 (blue dots). The conventional cosmological parameters are shown in the first two rows for the ΛCDM and scaling-DE models, and in the next two rows for the spike-DE models. The free dark energy parameters of the spike-DE models (A, B, σ) are shown in the bottom panels. The solid horizontal line in all panels represents the minimum chi-square value for the best-fit ΛCDM model (see Table I).

the Markov chain Monte Carlo (MCMC) chains are not easily converged due to multiple local maxima in the multidimensional likelihood distribution. Figure 3 presents chi square versus free model parameters from the *unconverged* trial MCMC chains of spike-DE models with three different values of $\log_{10} a_c = -4.5, -3.5$, and -2.5, showing how the preferred ranges of parameters change depending on the temporal position of the dark energy spike. For comparison, the results of the scaling-DE and ΛCDM models are also shown (top two rows). For the dark energy parameters (bottom panels), the priors are set as $0 \le A \le 0.6$, $0 \le B \le 0.01$, and $10^{-5} \le \sigma \le 0.1$. For the spike-DE model with $\log_{10} a_c = -4.5$, wide ranges of the dark energy parameters are preferred, allowing for a strong dark energy spike with a long duration ($A \lesssim 0.6$, $B \lesssim 0.01$, $\sigma \lesssim 0.1$). The ranges of the conventional cosmological parameters (shown in the third and fourth rows) are very similar to those of the ΛCDM model (top two rows). For the case of $\log_{10} a_c = -2.5$, the weaker dark energy spike with a shorter duration is favored ($A \lesssim 0.1$, $B \lesssim 0.01$, $\sigma \lesssim 0.03$). In both cases, however, the chi-square values are larger than the ΛCDM best-fit value, implying no improvement in the data fitting compared with the ΛCDM model. On the other hand, the spike-DE model with $\log_{10} a_c = -3.5$ prefers the presence of a dark energy spike with intermediate strength and a narrower width ($A \lesssim 0.4$, $B \lesssim 0.002$, $\sigma \lesssim 0.01$), providing improved fits to the data for several groups of dark energy parameters. In particular, around $(A, B, \sigma) = (0.28, 10^{-4}, 1.5 \times 10^{-3})$ or $(0.38, 5 \times 10^{-4}, 1.2 \times 10^{-3})$, the chi-square values are quite smaller than that of the ΛCDM best-fit model. We note that near these parameter groups, the preferred ranges

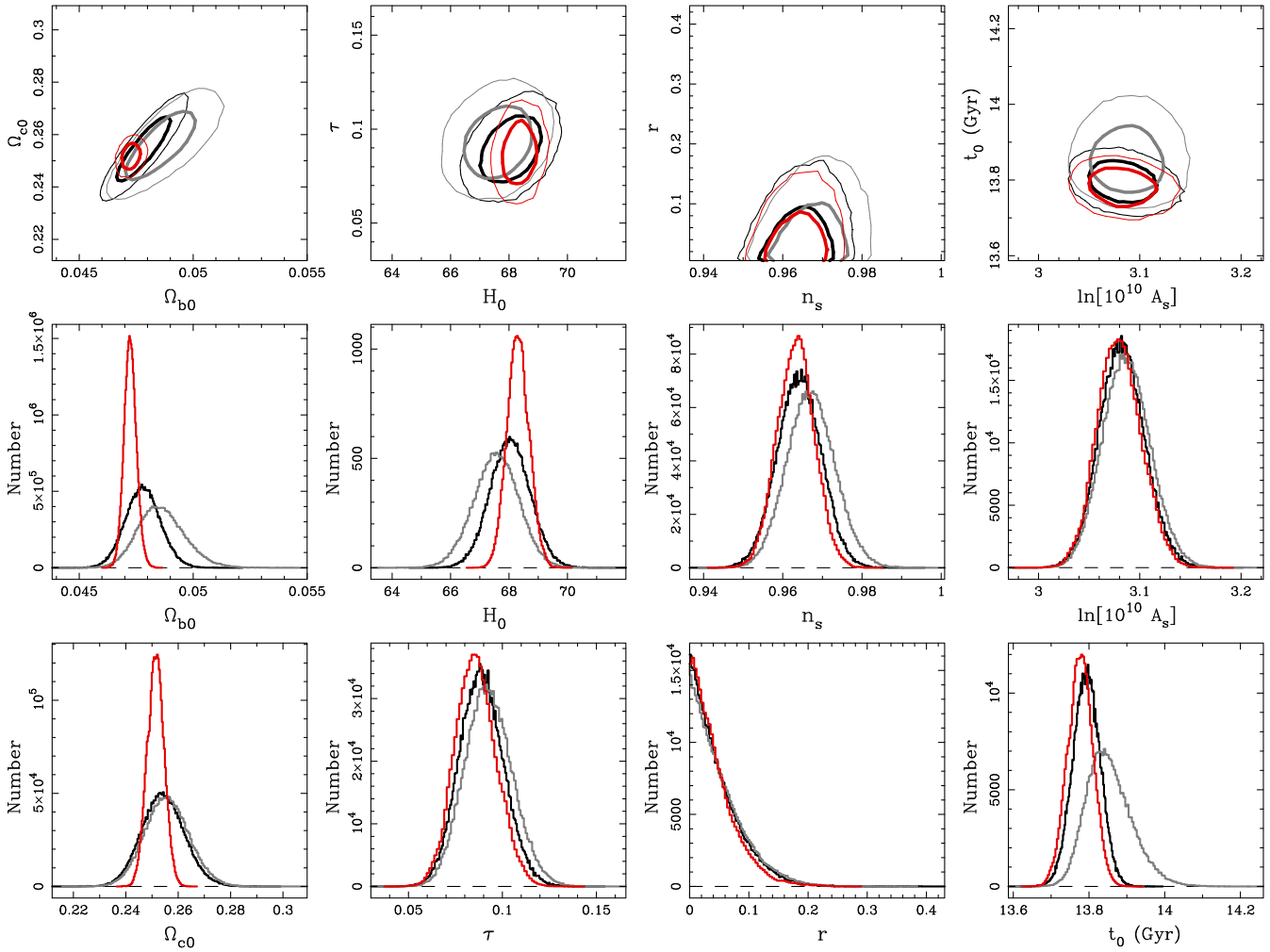

FIG. 4 (color online). Top: Two-dimensional likelihood contours of the conventional cosmological parameters favored by the Planck CMB and BAO data sets for the spike-DE (red), scaling-DE (grey), and ΛCDM (black curves) models. For the spike-DE model, the dark energy parameters have been fixed with the values given in Table I. The thick and thin solid curves indicate the 68.3% and 95.4% confidence limits, respectively. Middle and bottom: Marginalized one-dimensional likelihood distributions for each cosmological parameter, with arbitrary normalizations.

of the conventional cosmological parameters differ from those of the ΛCDM model; for example, a smaller baryonic matter density (Ω_{b0}) seems to be favored in this spike-DE model. Although the results are based on an incomplete MCMC analysis, they validate our choice of $\log_{10} a_c = -3.5$ to search for the dark energy model favored by observations over the ΛCDM model.

In this work, instead of obtaining the full converged MCMC chains for all of the free parameters, we search for the best-fit location in the likelihood distribution by manually running the `CosmoMC` with the option `action = 2` starting at the local maxima found from the trial MCMC chains (shown in Fig. 3) in the case of $\log_{10} a_c = -3.5$. The results are summarized in Table I, which lists the parameters of the ΛCDM, scaling-DE, and spike-DE models that best describe the observational data, together with the cosmic age (t_0) and the parameters related with foregrounds and instrumental calibrations.

To see how the conventional cosmological parameters are affected by the presence of the dark energy spike, we apply the MCMC method to randomly explore the parameter space that is favored by observations. For the spike-DE model, we have fixed the dark energy parameters A, B, and σ with the best-fit values given in Table I. For the scaling-DE model, however, the parameter B (the initial level of early dark energy) has been varied freely. Figure 4 shows two-dimensional likelihood contours and marginalized one-dimensional likelihood distributions of the conventional cosmological parameters favored by the Planck CMB and BAO data sets for the spike-DE, scaling-DE, and ΛCDM models, estimated from the converged MCMC chains. Note that here we present the likelihood distributions of Ω_{b0} and Ω_{c0} instead of $\Omega_{b0}h^2$ and $\Omega_{c0}h^2$. Table II summarizes the mean and 68.3% confidence limit of the cosmological parameters estimated from the one-dimensional likelihood distributions. For the tensor-to-scalar ratio r and the level of early dark energy B, the upper limits (95.4%) are given. Interestingly, compared with the ΛCDM model, the spike-DE model gives narrower parameter constraints on the baryon and CDM density parameters and the Hubble constant with standard deviations that are smaller by a factor of 2.8, 2.5, and 1.9, respectively, and best-fit values that slightly deviate from those of the ΛCDM model. Since the likelihoods of the spike-DE model sufficiently overlap with the ΛCDM ones, the estimated parameters of both models are still consistent with each other.

For the scaling-DE model, the parameter constraints are consistent with those of the ΛCDM model, except for slightly larger values of the baryon density and cosmic age. In this model we have set B as a free parameter to constrain the level of early dark energy density ($\Omega_e = B$). The allowed range for the early dark energy is $\Omega_e < 0.0045$ (95.4% confidence limit), which is narrower than the Planck constraint on the fluid-based early dark energy density parameter of Doran and Robbers [34] ($\Omega_e < 0.009$ [2]). Recently, a substantial improvement on the constraint $\Omega_e < 0.0036$ (at the 95% confidence level) has been obtained by the Planck 2015 data analysis [35].

IV. MODEL COMPARISON

In this section, we compare the best-fit ΛCDM, scaling-DE, and spike-DE models to see which model is preferred by the current observations based on statistical criteria, such as the likelihood ratio test and the Akaike and Bayesian information criteria that are widely used in the model selection.

TABLE II. Mean and standard deviation (68.3% confidence limit) of the conventional cosmological parameters estimated from the marginalized one-dimensional likelihood distribution for the best-fit ΛCDM, scaling-DE, spike-DE models constrained with the Planck CMB and BAO data sets. For the tensor-to-scalar ratio r and the level of early dark energy B, the upper limits (95.4%) are presented.

Parameter	ΛCDM	Scaling-DE	Spike-DE
$100\Omega_{b0}$	4.784 ± 0.076	4.869 ± 0.102	4.728 ± 0.027
Ω_{c0}	0.2547 ± 0.0081	0.2563 ± 0.0084	0.2518 ± 0.0032
h	0.6807 ± 0.0069	0.6761 ± 0.0077	0.6836 ± 0.0037
τ	0.090 ± 0.012	0.094 ± 0.013	0.087 ± 0.011
n_s	0.9644 ± 0.0056	0.9675 ± 0.0061	0.9638 ± 0.0047
r	< 0.130	< 0.138	< 0.120
$\ln[10^{10}A_s]$	3.084 ± 0.022	3.089 ± 0.024	3.083 ± 0.021
t_0 (Gyr)	13.795 ± 0.036	13.858 ± 0.060	13.781 ± 0.033
B	⋯	< 0.0045	⋯

TABLE III. Chi-square (χ^2) values of the best-fit ΛCDM, scaling-DE, and spike-DE models, together with differences of the chi square ($\Delta\chi^2$), Akaike information criterion (ΔAIC), and Bayesian information criterion (ΔBIC) relative to the ΛCDM value, and p-values estimated from the LRT statistic.

Data	ΛCDM	Scaling-DE	Spike-DE
`Lowlike`	2014.578	2014.178	2014.092
`Commander`	−7.304	−7.471	−8.096
`CamSpec`	7795.773	7796.223	7777.669
`Lensing`	9.892	9.190	9.881
DR7	0.858	0.620	0.439
DR9	0.431	0.603	0.812
6dF	0.019	0.034	0.036
Wiggle Z	0.047	0.024	0.021
Total χ^2	9814.295	9813.400	9794.753
$\Delta\chi^2$	…	−0.895	−19.542
p-value (LRT)	⋯	0.3441	6.148×10^{-4}
ΔAIC	⋯	1.105	−11.542
ΔBIC	⋯	6.982	11.968

Table III lists the separate chi-square (χ^2) values for each likelihood data set used in the parameter estimation for the best-fit ΛCDM, scaling-DE, and spike-DE models (see Table I for the best-fit values). The negative chi-square values for Commander likelihood data appear due to the arbitrary normalization of the log-likelihood in the CosmoMC software [36]. We note that the best-fit cosmological parameters in the presence of a dark energy spike near the radiation-matter equality gives a far smaller chi-square value than those of the ΛCDM model by about 5 times the number of new free parameters of the spike-DE model (A, B, $\log_{10} a_c$, σ), with a difference $\Delta\chi^2 \equiv \chi^2 - \chi^2_{\Lambda\mathrm{CDM}} = -19.542$, which is a significant improvement of the data fit.

The three dark energy models considered here are nested in the sense that the ΛCDM and scaling-DE models are special cases of the spike-DE model. In this case, we can apply the likelihood ratio test (LRT) as a model selection method, where the null model is the ΛCDM model and the alternative model is the scaling-DE or spike-DE model [4,12]. The test statistics is defined as twice the natural logarithm of the ratio of likelihoods of the null and alternative hypotheses (models) and is equivalent to the difference of the chi square relative to the ΛCDM one,

$$Q = 2\ln\frac{\mathcal{L}(H_{\Lambda\mathrm{CDM}}|D)}{\mathcal{L}(H|D)} = \Delta\chi^2, \tag{7}$$

where $\mathcal{L}(H|D)$ indicates the maximum likelihood of the alternative model (H) given the data (D), and likewise for the null model ($H_{\Lambda\mathrm{CDM}}$). The LRT statistic is a computationally cheap version of the Bayes factor which provides a criterion for penalizing models with more parameters based on the Bayesian theory [10]. The test statistic Q can be approximated as the χ^2 distribution with the degrees of freedom (d.o.f.) defined as the additional number of parameters of the nesting model (d.o.f. $= 4$ for the spike-DE model, and d.o.f. $= 1$ for the scaling-DE model). The p-value, the probability that the null hypothesis is supported by the observational data over the alternative one, is calculated from the cumulative χ^2 distribution and presented in Table III. We find that the p-value for the spike-DE model as an alternative is quite small ($p = 6.1 \times 10^{-4}$), suggesting a strong preference for the spike-DE model over the ΛCDM model.

The Akaike information criterion (AIC) is defined as [5,7,12]

$$\mathrm{AIC} = -2\ln\mathcal{L} + 2k, \tag{8}$$

where k is the number of free parameters of the model considered. If the alternative model gives a smaller AIC compared with the null (ΛCDM) model, it is ranked as a better model because the discrepancy with the true model is considered to be smaller. It is generally accepted that an AIC difference of 5 or more gives strong evidence supporting the model with the smaller AIC value (see Ref. [8] for the reliability of the AIC method in cosmological model selection). The differences of the AIC relative to the ΛCDM model ($\Delta\mathrm{AIC} = \Delta\chi^2 + 2$ d.o.f.) are listed in Table III. The scaling-DE model has a positive value of $\Delta\mathrm{AIC} = 1.1$, which means that introducing the scaling dark energy without a spike into the ΛCDM model does not improve the fit much. On the other hand, the negative value of $\Delta\mathrm{AIC} = -11.5$ for the spike-DE model suggests that the alternative model of dark energy with early scaling behavior and a dark energy spike (near the radiation-matter equality) is strongly favored by the current cosmological observations over the ΛCDM model.

As an alternative to the AIC, the Bayesian information criterion (BIC) is often used for model selection, which assigns a conservative penalty for a large sample size. The BIC is defined as [6,7,12]

$$\mathrm{BIC} = -2\ln\mathcal{L} + k\ln N, \tag{9}$$

where N is the number of data points. We set $N = 2637$ for Planck+BAO data sets ($31 \times 4 + 48 + 2451 + 8 + 6$ for Lowlike [TT, TE, EE, BB], Commander, CamSpec, lensing, and BAO data, respectively) to calculate the difference of the BIC relative to the ΛCDM value ($\Delta\mathrm{BIC} = \Delta\chi^2 + \mathrm{d.o.f.}\ln N$), which are listed in Table III. Contrary to the AIC result, the spike-DE model has a positive value of $\Delta\mathrm{BIC} = 12.0$. The strong evidence supporting the presence of a dark energy spike by the AIC has disappeared, since the BIC penalizes complex models due to the large number of data points, as in the CMB observation. In the context of the BIC, the scaling-DE model with d.o.f. $= 1$ is preferred over the spike-DE model (d.o.f. $= 4$).

In summary, a comparison of the maximum likelihoods of the spike-DE and ΛCDM models according to the LRT and AIC suggests that the spike-DE model is strongly preferred over the ΛCDM one, while the BIC still indicates that the observational data supports the simple ΛCDM model over others. From the definitions of the AIC and BIC, we see that the AIC is inclined to select the model that better fits the data, while the BIC selects a simpler model with less parameters. Apart from the model selection between the ΛCDM and spike-DE models, we at least conclude that the spike-DE model fits the observational data far better than the ΛCDM model with the different cosmological parameter estimation.

According to Table III, the spike-DE model improves fitting to the CamSpec high-ℓ temperature likelihood data. Figure 5 verifies that the chi-square decrease is mainly due to the better fitting of the Planck temperature power spectrum data around the third ($\ell \approx 800$) and sixth ($\ell \approx 1800$) acoustic peaks, where strong residuals relative to the best-fit ΛCDM model are seen. In the middle and

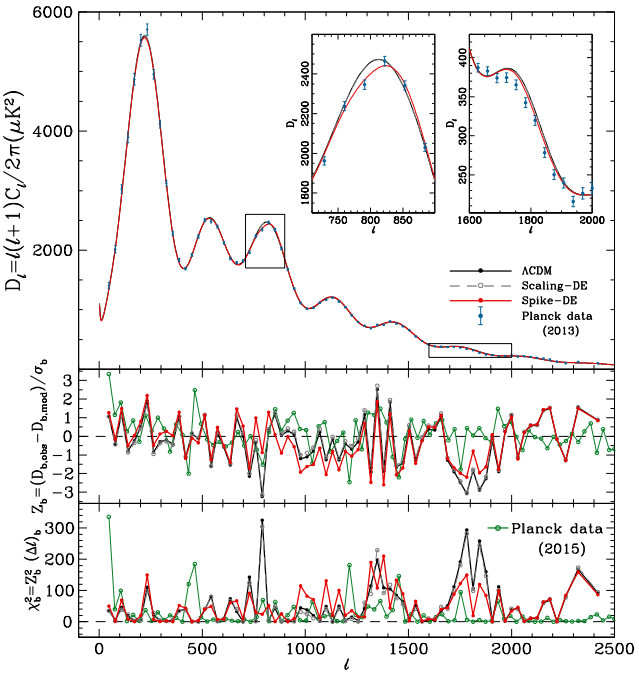

FIG. 5 (color online). Top: The CMB temperature angular power spectra of the best-fit ΛCDM (black), scaling-DE (grey), and spike-DE models (red curves). The angular power spectrum is given as $D_\ell = \ell(\ell+1)C_l/(2\pi)$ in $\mu\mathrm{K}^2$ units. The Planck 2013 data points are shown as blue dots with error bars. The insets magnify the regions of $\ell \approx 800$ and 1800. Middle and bottom: The difference between observation and the best-fit model prediction of the band power divided by the measurement error (σ_b) for each ℓ bin (denoted as b), $Z_b = (D_{b,\mathrm{obs}} - D_{b,\mathrm{mod}})/\sigma_b$, and the sum of the contribution due to Z_b^2 within the bin, $\chi_b^2 = Z_b^2(\Delta\ell)_b$. For comparison, the quantities Z_b and χ_b^2 estimated from the Planck 2015 data and the best-fit ΛCDM model prediction (constrained with Plank 2015 TT + LowP + Lensing data) are presented (green open circles [3]).

bottom panels of Fig. 5, we plot the difference of the observed and model-predicted band power spectra (D_b) normalized with the measurement error (σ_b) for each ℓ bin (here denoted as b), $Z_b = (D_{b,\mathrm{obs}} - D_{b,\mathrm{mod}})/\sigma_b$, and the sum of the contribution due to Z_b^2 within the bin, $\chi_b^2 \equiv Z_b^2(\Delta l)_b$, which approximates the chi-square contribution for each bin. The model band power $D_{b,\mathrm{mod}}$ is the average of the CMB angular power spectrum $D_\ell = \ell(\ell+1)\times C_\ell/(2\pi)$ predicted by a model within a specified bin. We use the same ℓ bins that were used in the Planck team's analysis. It was originally reported that the strong residuals seen around the third ($\ell \approx 800$) and fifth ($\ell \approx$ 1300–1500) acoustic peaks are real features of the primordial CMB sky [2]. We note that the best-fit spike-DE model significantly alleviates the strong residuals around the third ($\ell \approx 800$) and sixth ($\ell \approx 1800$) acoustic peaks observed in the best-fit ΛCDM model (red and black dots). However, the residual around the fifth peak ($\ell \approx$ 1300–1500) still remains in both models.

V. DISCUSSION AND CONCLUSION

In this paper, we investigated the observational effect of early episodically dominating dark energy which accommodates a dark energy spike—a sudden transient variation in dark energy density—together with early scaling behaviors and late-time acceleration.

The dark energy model with a spike (spike-DE model) near the radiation-matter equality era improves the fit to the Planck CMB temperature power spectrum data around the third ($\ell \approx 800$) and sixth ($\ell \approx 1800$) acoustic peaks. Comparing the likelihood distributions based on the maximum likelihood ratio test and the Akaike information criterion as the statistical model selection methods, we found that the spike-DE model is strongly favored by observations over the conventional ΛCDM model. Furthermore, the spike-DE model provides a different cosmological parameter estimation with tighter constraints on the matter density and Hubble constant (see Fig. 4 and Table II). However, the strong evidence supporting the presence of the dark energy spike disappears based on the Bayesian information criterion, which assigns a conservative penalty to a model with a large number of parameters.

We have checked that including high-ℓ CMB data observed by the South Pole Telescope and the Atacama Cosmology Telescope [37,38] or excluding the tensor-type perturbation do not affect our main results. Besides, we inferred that the foreground and instrumental calibration parameters do not play a major role in improving the fit to the data. If they do, a significant reduction of the chi square should be seen in the case of the ΛCDM model, too.

Very recently, the Planck 2015 data were made publicly available. The main scientific conclusions of the Planck 2015 data analysis are consistent with the previous results, with cosmological parameters deviating by less than 0.7σ [3]. As shown in Fig. 5, the strong residuals around $\ell \approx 800$ and $\ell \approx 1800$ in the Planck 2013 temperature power spectrum data are not observed in the Planck 2015 data; the deviation from the best-fit ΛCDM model prediction becomes much smaller (see green open circles in the middle and bottom panels of Fig. 5). Therefore, the success of the spike-DE model in improving the fit to the Planck 2013 temperature power spectrum in these regions is no longer expected in the recent Planck 2015 data. However, the presence of strong residuals at $\ell = 400$–500 and $\ell \approx 1200$ in the Planck 2015 data still leaves open the possibility that the new data are fitted by another candidate model of dark energy far better than the ΛCDM model.

Through an example of the dark energy spike model, we emphasized that the alternative cosmological parameter estimation is allowed in Einstein's gravity, with an even better fitting of the same observational data than the conventional ΛCDM model.

ACKNOWLEDGMENTS

The author would like to thank Professor Jai-chan Hwang for valuable discussions. C. G. P. was supported by the Basic Science Research Program through the National Research Foundation of Korea (NRF) funded by the Ministry of Science, ICT and Future Planning (No. 2013R1A1A1011107).

[1] G. Hinshaw *et al.* (WMAP Collaboration), Astrophys. J. Suppl. Ser. **208**, 19 (2013).
[2] P. A. R. Ade *et al.* (Planck Collaboration), Astron. Astrophys. **571**, A16 (2014).
[3] P. A. R. Ade *et al.* (Planck Collaboration), arXiv: 1502.01589.
[4] J. Neyman and E. S. Pearson, Phil. Trans. R. Soc. A **231**, 289 (1933); S. S. Wilks, Ann. Math. Stat. **9**, 60 (1938).
[5] H. Akaike, IEEE Trans. Autom. Control **19**, 716 (1974).
[6] G. Schwarz, Ann. Stat. **6**, 461 (1978).
[7] A. R. Liddle, Mon. Not. R. Astron. Soc. **351**, L49 (2004).
[8] M. Y. J. Tan and R. Biswas, Mon. Not. R. Astron. Soc. **419**, 3292 (2012).
[9] A. F. Heavens, T. D. Kitching, and L. Verde, Mon. Not. R. Astron. Soc. **380**, 1029 (2007).
[10] T. D. Saini, J. Weller, and S. L. Bridle, Mon. Not. R. Astron. Soc. **348**, 603 (2004).
[11] G. Efstathiou, Mon. Not. R. Astron. Soc. **388**, 1314 (2008).
[12] M. Szydlowski, A. Krawiec, A. Kurek, and M. Kamionka, Eur. Phys. J. C **75**, 5 (2015).
[13] A. R. Liddle, P. Mukherjee, D. Parkinson, and Y. Wang, Phys. Rev. D **74**, 123506 (2006).
[14] M. C. March, G. D. Starkman, R. Trotta, and P. M. Vaudrevange, Mon. Not. R. Astron. Soc. **410**, 2488 (2011).
[15] P. Serra, A. Heavens, and A. Melchiorri, Mon. Not. R. Astron. Soc. **379**, 169 (2007).
[16] M. Biesiada, B. Malec, and A. Piórkowska, Res. Astron. Astrophys. **11**, 641 (2011).
[17] A. Borowiec, W. Godlowski, and M. Szydlowski, Int. J. Geom. Methods Mod. Phys. **04**, 183 (2007).
[18] A. De Felice, S. Nesseris, and S. Tsujikawa, J. Cosmol. Astropart. Phys. 05 (2012) 029.
[19] S. del Campo, J. C. Fabris, R. Herrera, and W. Zimdahl, Phys. Rev. D **83**, 123006 (2011).
[20] Y. Gong, X.-m. Zhu, and Z. H. Zhu, Mon. Not. R. Astron. Soc. **415**, 1943 (2011).
[21] J. Lu, L. Xu, J. Li, B. Chang, Y. Gui, and H. Liu, Phys. Lett. B **662**, 87 (2008).
[22] C.-G. Park, J.-h. Lee, J.-c. Hwang, and H. Noh, Phys. Rev. D **90**, 083526 (2014).
[23] A. Lewis and A. Lasenby, Astrophys. J. **513**, 1 (1999); A. Lewis, A. Challinor, and A. Lasenby, Astrophys. J. **538**, 473 (2000).
[24] A. Lewis and S. Bridle, Phys. Rev. D **66**, 103511 (2002).
[25] W. Hu and I. Sawicki, Phys. Rev. D **76**, 104043 (2007); W. Hu, Phys. Rev. D **77**, 103524 (2008); W. Fang, S. Wang, W. Hu, Z. Haiman, L. Hui, and M. May, Phys. Rev. D **78**, 103509 (2008); W. Fang, W. Hu, and A. Lewis, Phys. Rev. D **78**, 087303 (2008).
[26] An ESA science mission with instruments and contributions directly funded by ESA Member States, NASA, and Canada; http://www.esa.int/Planck.
[27] G. Hinshaw *et al.*, Astrophys. J. Suppl. Ser. **208**, 19 (2013).
[28] P. A. R. Ade *et al.* (Planck Collaboration), Astron. Astrophys. **571**, A15 (2014).
[29] P. A. R. Ade *et al.* (Planck Collaboration), Astron. Astrophys. **571**, A17 (2014).
[30] N. Padmanabhan, X. Xu, D. J. Eisenstein, R. Scalzo, A. J. Cuesta, K. T. Mehta, and E. Kazin, Mon. Not. R. Astron. Soc. **427**, 2132 (2012).
[31] L. Anderson *et al.*, Mon. Not. R. Astron. Soc. **427**, 3435 (2012).
[32] F. Beutler, C. Blake, M. Colless, D. Heath Jones, L. Staveley-Smith, L. Campbell, Q. Parker, W. Saunders, and F. Watson, Mon. Not. R. Astron. Soc. **416**, 3017 (2011).
[33] C. Blake *et al.*, Mon. Not. R. Astron. Soc. **425**, 405 (2012).
[34] M. Doran and G. Robbers, J. Cosmol. Astropart. Phys. 06 (2006) 026.
[35] P. A. R. Ade *et al.* (Planck Collaboration), arXiv:1502.01590.
[36] http://cosmocoffee.info/viewtopic.php?t=2216.
[37] R. Keisler *et al.*, Astrophys. J. **743**, 28 (2011).
[38] S. Das *et al.*, J. Cosmol. Astropart. Phys. 04 (2014) 014.